informatics

Article

The Design and Development of a Foot-Detection Approach Based on Seven-Foot Dimensions: A Case Study of a Virtual Try-On Shoe System Using Augmented Reality Techniques

Charlee Kaewrat [1,2], Poonpong Boonbrahm [1,2] and Bukhoree Sahoh [1,2,*]

1 School of Informatics, Walailak University, Tha Sala, Nakhon Si Thammarat 80160, Thailand; charlee.ke@wu.ac.th (C.K.); bpoonpon@wu.ac.th (P.B.)
2 Informatics Innovation Center of Excellence (IICE), Walailak University, Tha Sala, Nakhon Si Thammarat 80160, Thailand
* Correspondence: bukhoree.sa@wu.ac.th

Abstract: Unsuitable shoe shapes and sizes are a critical reason for unhealthy feet, may severely contribute to chronic injuries such as foot ulcers in susceptible people (e.g., diabetes patients), and thus need accurate measurements in the manner of expert-based procedures. However, the manual measure of such accurate shapes and sizes is labor-intensive, time-consuming, and impractical to apply in a real-time system. This research proposes a foot-detection approach using expert-like measurements to address this concern. It combines the seven-foot dimensions model and the light detection and ranging sensor to encode foot shapes and sizes and detect the dimension surfaces. The graph-based algorithms are developed to present seven-foot dimensions and visualize the shoe's model based on the augmented reality (AR) technique. The results show that our approach can detect shapes and sizes more effectively than the traditional approach, helps the system imitate expert-like measurements accurately, and can be employed in intelligent applications for susceptible people-based feet measurements.

Keywords: feet measurement; foot recognition; diabetic foot; digital healthcare; LiDAR sensor; real-time monitoring; feature extraction; diabetic foot ulcer; computer-aided analysis

Citation: Kaewrat, C.; Boonbrahm, P.; Sahoh, B. The Design and Development of a Foot-Detection Approach Based on Seven-Foot Dimensions: A Case Study of a Virtual Try-On Shoe System Using Augmented Reality Techniques. *Informatics* **2023**, *10*, 48. https://doi.org/10.3390/informatics10020048

Academic Editor: Long Jin

Received: 21 April 2023
Revised: 31 May 2023
Accepted: 2 June 2023
Published: 5 June 2023

1. Introduction

Healthy feet are the main factor for activity in daily life, whether in movement related to work or exercise [1]. Neglecting foot health may result in chronic injuries such as foot ulcers [2]. It is a significant obstacle for susceptible people who are suffered from negative long-term consequences and substantial healthcare expenses [3].

Suitable shoe shapes and sizes are essential for healthy feet and need accurate measurements. Available shoes in the commercial sectors are based on the average size, standardizing the foot base on a measuring tape (length and width). It may not be comfortable and nor fit for susceptible people such as diabetes patients [4]. Moreover, manually finding shoe sizes is tedious and time-consuming [5]. Therefore, optical measuring technologies, binocular vision, phase measurement, digital holography, and structured light techniques have become the principal machine measures for mass-customized shoes; however, detecting foot characteristics is a complex process [6]. In this way, 3D-scanning-based technology has been extensively investigated in computer graphics to address that concern [7]. It employs a laser-based technique to detect foot shape and identify size by releasing reflected light on a foot's surface, that can then accurately compute to produce a virtual item [8].

However, accessing high-quality technologies is difficult for ordinary patients since their cost is very high, and the measurement procedure may take a very long time. Some research has attempted to overcome this limitation by proposing simple 3D-scanning devices based on RGB-depth cameras such as PrimeSense, Kinect, and RealSense. Compared to conventional 3D scanning equipment, they are affordable, portable, and simple to operate [9]. In addition, some of them apply visualization-based try-on simulations as assistive tools to help people measure foot size in order to make better decisions [10]. The visualization may utilize AR technology to manufacture relevant foot information based on smart devices. For instance, Jiang et al. proposed an AR-based approach for the virtual try-on of shoes projected on mobile devices [11]. They found that a detection system, applied to the AR technique and displayed on mobile devices, helps people effectively enhance their perception of a product.

The principals of feet detection technology consist of two main processes: (1) the information detection process and (2) the information visualization process. It may begin with a detection process based on the marker-based process that senses real-time signals from the real-world environment and extracts essential information. The results let computer systems simultaneously simulate virtual objects based on 3D models mixed with real-world objects. Technically, there are two well-known approaches for foot detection systems. Firstly, the marker-based sensing approach uses a physical symbol (such as photos or text) as a reference position using an RGB camera [12]. The current systems focus on simulating virtual foot measurements using the marker-based approach to track and monitor objects [13]. However, this technique depends on the quality of the marker positions that are placed on unmoving objects unsuitable for detecting active objects, such as the human body. It becomes a limitation when users, such as diabetes patients, need accurate foot measurements, but cannot access advanced and professional tools. Secondly, the markerless-based sensing approach utilizes the feature of a depth camera for real-time object tracking, which can also apply to foot-detection systems. Addressing this concern, by introducing a new markerless-based approach to the standard of professional tools that can be accessed through mobile devices so that ordinary people can accurately measure their shoe size at anytime and anywhere, is challenging.

This research proposes a foot-detection system based on the markerless-based AR approach. It is a novel approach that is empowered by seven-foot dimensions techniques to imitate expert-based measurement procedures. The main contributions are:

- To propose a new system architecture for a feet detection approach based on markerless-based AR techniques that let ordinary people applicably measure their feet to an expert standard.
- To design and develop the foot-detection approach using markerless techniques based on seven-foot dimensions, measuring and visualizing shoe sizes accurately in a user-friendly manner.
- To prove that the proposed markerless-based approach based on seven-foot dimensions helps the system measure and visualize shoe sizes, and converge towards expert-based procedures.

The real-time-based systems for foot detection are examined in Section 2. The overview system architecture of the proposed system is discussed in Section 3. Section 4 concentrates on the design and methodology of the foot-detection system, with Section 5 evaluating the approach's effectiveness based on seven-foot dimensions based on quantitative experiments. Conclusions and future directions appear in Section 6.

2. Related Works

This section examines the foot-detection approach based on the need for its accurate analysis of susceptible individuals, such as chronic patients and older people. Furthermore, the application of expert-based measurements and real-time technologies to estimate foot shape and size is considered in order to reveal the research gap of recent foot-detection systems.

2.1. Feet Detection

The susceptible people are those whose feet are sensitive to injury caused by unfitted footwear that may affect long-term foot health, such as chronic patients and older people [14]. Alsheikh et al. [15] researched the need for primary healthcare based on diabetic foot conditions. They found that, recently, patients have been less cared for in terms of foot health and that there is a need for further study to fill this gap. This suggests that utilizing advanced technologies is challenging but may alleviate this problem.

Researchers have addressed this concern based on machine learning techniques. D'Angelo et al. [16] proposed an approach for foot detection using interpretable machine learning techniques. They discussed how the approach could explain the problem explicitly, allowing staff to understand the foot condition and effectively decide on the treatment. Thotad et al. [17] and Ahsan et al. [18] proposed an approach for detecting diabetic foot ulcers using deep learning and computer vision techniques. They discussed the proposed techniques to help the system detect foot ulcers effectively. Some have solved the problem using sensor technologies to detect the foot shape and size. Mei [19] and Kini et al. [20] employed force sensors that measure and classify foot types and that allow the system to match each foot with proper footwear. They claimed that the techniques help people choose suitable footwear and may prevent long-term negative effects. In addition, Chun et al. [21] proposed a foot-detection approach using an RGB-D camera as a sensor. They emphasized the foot arch details critical for measuring and capturing the fit size and shape factors. They concluded that they produced high-quality inputs that effectively let the system analyze foot arch characteristics.

Although numerous studies have proposed new approaches to deal with foot measurement problems with high detection effectiveness, none consider the already-used approaches for real-time foot measuring at home with user-friendly devices. They employed high computational performance, sensors, and techniques that are not yet ready to deploy for ordinary patients who are not experts. Moreover, they focused on post-event analysis rather than on an assistive tool for patients to measure appropriate footwear shapes and sizes in order to prevent worse cases. This research gap is challenging, but it may be possible to apply lightweight sensors with real-time technologies to address this concern.

2.2. Foot Detection Based on Real-Time-Based System

A foot-detection technique based on a real-time system aims to estimate the shape size so that people can choose suitable shoes. It connects physical and computer-generated objects in a virtual environment, letting people envision the approximate shoes fitted to their personalities. It may employ online processing to produce a live-stream simulation of foot information in particular situations. AR offers a real-time-based system for foot detection that lets systems control the real-world environment and interact with 3D-based virtual objects; however, applying AR to automatic foot detection in medical fields is challenging [22].

Research has examined AR technologies to support real-time-based systems and has primarily been relevant to medical training [23]. Focusing on health care, Sip et al. [24] and de Assis et al. [25] proposed AR-based systems as assistive tools to help staff rehabilitate patients affected by stroke. They discussed the fact that AR technologies let physicians and experts practice their readiness for first aid. Moreover, Jeung et al. [26] employed AR technologies to guide physicians in understanding surgical processes. They confirmed that AR technologies help them reduce faults during operations effectively. This suggests that AR technologies are in demand in medical fields, and that they can help physicians and experts deal with emergency cases. Unfortunately, most of the available studies introduce AR technologies in order to support experts, and few studies concern susceptible people, such as diabetes patients, who need technologies that measure their feet, both shape and size, and which they can try at home with available devices.

In conclusion, real-time foot-detection systems for ordinary people are currently in their infant stage and demand research that needs further contribution in order to address the knowledge gaps. We highlight recent research gaps in terms of two limitations: (1) a lack of study on lightweight sensors to measure foot shape based on available devices and (2) the absence of a proposed ground truth to measure and identify foot shape descriptions concerning diabetic patients. The following section will show the overview system architecture of real-time feet detection to address the challenges.

3. Overview Architecture of Proposed System

This overview of the system architecture aims to describe the feet identification procedures that begin with signal encoding, in order to transform them into a machine-readable format. It illustrates how real-time system processes represent foot size and shape based on the AR system framework. It consists of four sub-components: (1) data streaming, (2) dimensional transformation, (3) feet identification, and (4) feet representation, as shown in Figure 1.

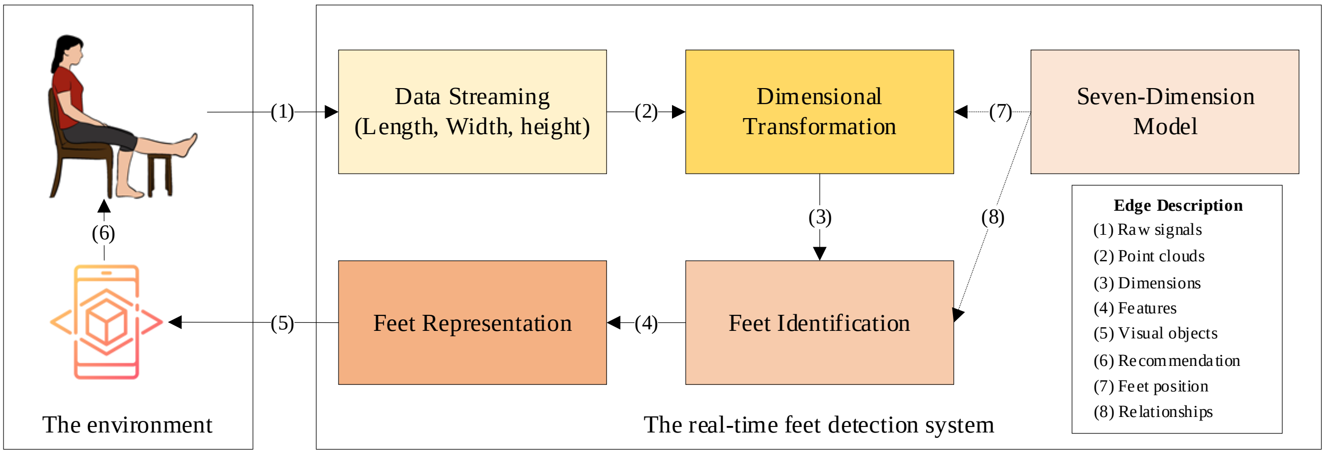

Figure 1. The overview system architecture for real-time foot detection based on AR techniques.

Figure 1 shows the overview architecture system that cycles between the real-world environment and the proposed system. The environment produces raw signals, collected by lightweight sensors, and inputs them into the system using the data-streaming component. Each raw signal transaction stores the object's surface-based three-dimensional (3D) objects (length, width, and height). The dimension transformation extracts relevant features, called a set of point clouds, according to the object's surface. Feet identification employs point clouds to connect their relationships and draw the shape and size of natural feet from the environment. Finally, feet representation visualizes feet information through graphical information that non-experts can employ through intelligent devices, which may help people understand the condition and make the right decision.

The challenging components in the architecture are dimension transformation and feet identification, because the effectiveness of real-time feet detection and usability depends on how the system can determine the foot shape and size. We propose the seven-dimension concept to model general feet from the raw signals that manufacture relevant point clouds and their relationships. This is a blueprint model that imitates expert-like measurement, and our system may identify dimensions in the same manner. Following this section, we aim to develop a seven-dimension model encoding to apply to the real-time foot detection system and usability based on AR techniques.

We will follow the overview system architecture to structure the rest of our study, and the following section will propose the design and development of the seven-dimension model.

4. Proposed Seven-Dimension Model

The effectiveness of our proposed system depends on how the dimension transformation and feet identification components can compute dimensions and features. Therefore, we propose a human-like encoding based on the seven-dimension model to recognize feet shapes and semantic relationships.

4.1. Feet Dimension Extraction

Feet detection needs dimensional information as a fundamental element in a computer system. A fixed template is a standard technique for measuring feet size. It matches feet and extracts dimensional information, and is a simple and handy measurement. The graphic template is shown in Figure 2.

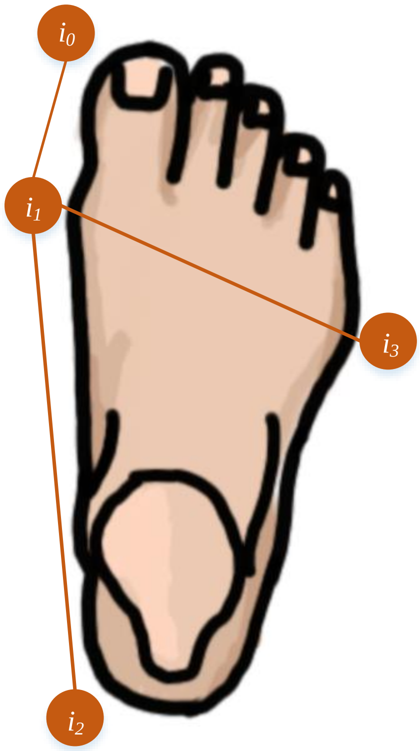

Figure 2. Basic foot template structures.

Figure 2 shows the template structures that identify foot size with length and width, transforming them into shape and size based on an average mean. The length is the distance between nodes i_0, i_1, and i_2, and the width is the distance between i_1 and i_3. Although it is straightforward for domain experts in industrial sectors to use the template, it cannot effectively define the foot shape in a real-time system. It requires an advanced technique to identify precise details such as foot thickness and heel breadth.

To fulfill the abovementioned limitations, we extend the template structure by encoding seven-foot dimensions to support feet shape extraction. Our proposed technique imitates how domain experts determine the feet dimensions that are needed in sensitive measurement cases such as in the medical field. We illustrate the extended template structures needed in the real-time foot detection system, as shown in Figure 3.

Figure 3 represents the foot dimensions needed in foot detection systems aligned with individual preferences. It considers foot shape, with depth and thickness being close to domain expert justifications. Each dimension provides a different impact on the user's individual preference that may define foot shape correctly. For instance, the "*Ball of foot length*" in Figure 3b helps the measurement process determine the lower part of shoes on the right-hand side, that is needed for challenging activities such as jogging. In other words, all dimensions offer vital roles in terms of foot measurement, and their descriptions and significance in seven-foot dimensions are shown in Table 1.

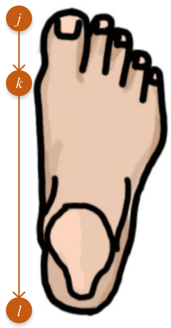

(**a**) Foot Length (FL)

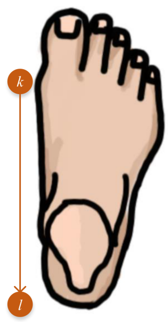

(**b**) Ball of foot length (BFL)

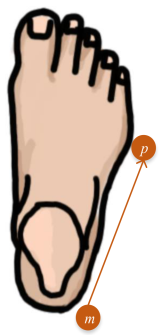

(**c**) Outside ball of foot length (OBFL)

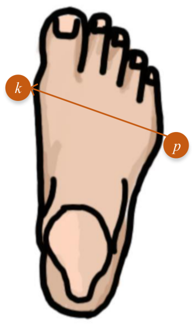

(**d**) Foot breadth diagonal (FBD)

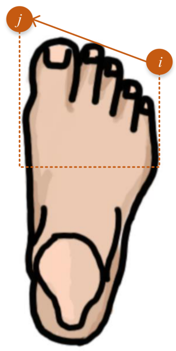

(**e**) Foot breadth horizontal (FBH)

(**f**) Heel breadth (HB)

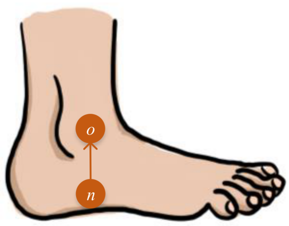

(**g**) Instep height (IH)

Figure 3. The extended template structures based on a seven-foot dimension model.

Table 1. The descriptions and significances of seven-foot dimensions.

Dimension	Algebraic Function	Description
$FL_{dimension}$	$FL_{dimension} = (FL_{ending}, FL_{beginning})$, $FL_{beginning} = f\ (x_{FL,\ beginning}, y_{FL,\ beginning}, z_{FL,\ beginning})$, $FL_{endending} = f\ (x_{FL,\ ending}, y_{FL,\ ending}, z_{FL,\ ending})$, $FL_{beginning}$ and $FL_{ending} \subseteq$ Point Clouds	This determines the curves that naturally fit with a real-size user's feet and plays an essential role in reducing exercise-related pain (e.g., running and jumping).
$BFL_{dimension}$	$BFL_{dimension} = (BFL_{ending}, BFL_{beginning})$, $BFL_{beginning} = f\ (x_{BL,\ beginning}, y_{BL,\ beginning}, z_{BL,\ beginning})$, $BFL_{ending} = f\ (x_{BL,\ ending}, y_{BL,\ ending}, z_{BL,\ ending})$, $BFL_{beginning}$ and $BFL_{ending} \subseteq$ Point Clouds	This extracts the foot axis between the end of the heel and the metatarsal tibial, reducing exercise-related pain (e.g., running and jumping).
$OBFL_{dimension}$	$OBFL_{dimension} = (OBFL_{ending}, OBFL_{beginning})$, $OBFL_{beginning} = f\ (x_{OBFL,\ beginning}, y_{OBFL,\ beginning}, z_{OBFL,\ beginning})$, $OBFL_{ending} = f\ (x_{OBFL,\ ending}, y_{OBFL,\ ending}, z_{OBFL,\ ending})$, $OBFL_{beginning}$ and $OBFL_{ending} \subseteq$ Point Clouds	A good measurement of this dimension helps prevent the causes of pain around the foot's outside, including the forefoot, midfoot, and heel.

Table 1. *Cont.*

Dimension	Algebraic Function	Description
$\text{FBD}_{\text{dimension}}$	$\text{FBD}_{dimension}$ = (FBD_{ending}, $\text{FBD}_{beginning}$), $\text{FBD}_{beginning} = f\ (x_{FBD,\,beginning}, y_{FBD,\,beginning}, z_{FBD,\,beginning})$, $\text{FBD}_{ending} = f\ (x_{FBD,\,ending}, y_{FBD,\,ending}, z_{FBD,\,ending})$, $\text{FBD}_{beginning}$ and $\text{FBD}_{ending} \subseteq$ Point Clouds	This extracts a measurement between a ball's metatarsal tibial and metatarsal fibular bones. This helps identify shoe designs based on a suitable shape curve.
$\text{FBH}_{dimension}$	$\text{FBH}_{dimension}$ = (FBH_{ending}, $\text{FBH}_{beginning}$), $\text{FBH}_{beginning} = f\ (x_{FBH,\,beginning}, y_{FBH,\,beginning}, z_{FBH,\,beginning})$, $\text{FBH}_{ending} = f\ (x_{FBH,\,ending}, y_{FBH,\,ending}, z_{FBH,\,ending})$, $\text{FBH}_{beginning}$ and $\text{FBH}_{ending} \subseteq$ Point Clouds	This determines suitable sizes based on the foot's horizontal breadth. This avoids fundamental problems, such as narrow and loose shoes, both of which may cause an accident.
$\text{HB}_{dimension}$	$\text{HB}_{dimension}$ = (HB_{ending}, $\text{HB}_{beginning}$), $\text{HB}_{beginning} = f\ (x_{HB,\,beginning}, y_{HB,\,beginning}, z_{HB,\,beginning})$, $\text{HB}_{ending} = f\ (x_{HB,\,ending}, y_{HB,\,ending}, z_{HB,\,ending})$, $\text{HB}_{beginning}$ and $\text{HB}_{ending} \subseteq$ Point Clouds	This measures the distance between the pterion point and the toe, called the heel size. It is an element to estimate the correct heel size that helps users walk and run properly.
$\text{IH}_{dimension}$	$\text{IH}_{dimension}$ = (IH_{ending}, IH_{begin}), $\text{IH}_{beginning} = f\ (x_{IH,\,beginning}, y_{IH,\,beginning}, z_{IH,\,beginning})$, $\text{IH}_{ending} = f\ (x_{IH,\,ending}, y_{IH,\,ending}, z_{IH,\,ending})$, $\text{IH}_{beginning}$ and $\text{IH}_{ending} \subseteq$ Point Clouds	This dimension helps define the foot arch (e.g., a low instep defines a flat arch, which defines the foot shape as a flat foot).

Table 1 shows the foot dimensions and their computational notations. Each dimension plays a crucial role in foot identification with semantic descriptions. It enables systems to determine foot parts based on 3D information that helps simulate visual objects close to real-world objects. For instance, foot length ($\text{FL}_{dimension}$) is an ordered pair that can be defined by $\text{FL}_{dimension}$ = (FL_{ending}, $\text{FL}_{beginning}$); each element of the pair is represented by 3D objects (length, width, and height) between FL_{ending} and $\text{FL}_{beginning}$ and they can be determined as follows:

$$\text{FL}_{beginning} = f\ (x_{FL,\,beginning}, y_{FL,\,beginning}, z_{FL,\,beginning}) \tag{1}$$

$$\text{FL}_{ending} = f\ (x_{FL,\,ending}, y_{FL,\,ending}, z_{FL,\,ending}) \tag{2}$$

Both equations represent ordered pairs in 3D dimensions (e.g., x, y, and z). For example, the $\text{FL}_{beginning}$ element consists of a group of $x_{FL,\,beginning}$ encoding the dimension length, a group of $y_{FL,\,beginning}$ encoding the dimension width, and a group of $z_{FL,\,beginning}$ encoding the dimension height. The $f\ (\ )$ computes the radius of the average element spacing of the points in cloud density and approximately represents the elements of the dimensions. The rest are modeled to support foot identification and allow the systems to determine foot dimensions in the manner of expert intelligence.

A lack of consideration of any of the elements may cause susceptible people to have trouble with their daily activities. However, each dimension cannot be employed independently to measure the foot shape; they must be integrated to identify the proper foot shape aligned with user preferences. In this way, determining the relationships between them is needed, and the following section will propose the semantic relationships process to attend to this requirement.

4.2. Feet Detection Based on Semantic Relationships

The foot detection component aims to recognize the relationships between the seven-foot dimensions. It represents semantic meanings, based on human understanding, to connect each dimension and perform the shape and size measurements. Feet detection employs a set of seven-foot dimensions, coordinated in ordered pairs (see Table 1). It lets systems compute and link each dimension using a graph-based representation $\boldsymbol{G} = (\boldsymbol{V}, \boldsymbol{E})$. $\boldsymbol{V}$ (vertices) models on seven-foot dimensions and $\boldsymbol{E}$ (edge) connect paired vertices that are stored in $\boldsymbol{G}$ (graph). The graphic representation of this is shown in Figure 3, where each dimension semantically relates to the other. This research proposes an algorithm to perform the G in Algorithm 1.

Algorithm 1 Feet Identification based on Semantic Relationships

Inputs: a set of seven-foot dimensions' coordinates, $C = \{((x_{1,\ beginning}, y_{1,\ beginning}, z_{1,\ beginning}), (x_{1,\ ending}, y_{1,\ ending}, z_{1,\ ending})), ((x_{2,\ beginning}, y_{2,\ beginning}, z_{2,\ beginning}), (x_{2,\ ending}, y_{2,\ ending}, z_{2,\ ending})), \ldots, ((x_{7,\ beginning}, y_{7,\ beginning}, z_{7,\ beginning}), (x_{7,\ ending}, y_{7,\ ending}, z_{7,\ ending}))\}$

Outputs: a graph of seven-foot dimensions, $G = (V, E)$

1. **add Graph** G = null
2. **set** $V = [\varnothing]$
3. **set** $E = [\varnothing]$
4. **for** $\left(C_{i,\ beginning}, C_{i,\ ending}\right)$ **in** C **do**
5. **set** $X = C_{i,\ beginning}$;
6. **set** $Y = C_{i,\ ending}$;
7. **if** X **in** V: **continue**;
8. **else add** X **to** V;
9. **end if**
10. **if** Y **in** V: **continue**;
11. **else add** Y **to** V;
12. **end if**
13. **if** (X, Y) **in** E: **continue**;
14. **else add** $X \rightarrow Y$ **to** V;
15. **end if**
16. **end for**
17. **add node** V **to** G;
18. **add edge** E **to** G;
19. **return** G;

Algorithm 1 expresses the semantic-based rules to connect the nodes based on a pre-defined model, employing the graph-based index. C encodes a set of ordered pairs of foot dimension coordinates between $C_{i,\ beginning}$ and $C_{i,\ ending}$ (see in lines 4–9). The i indexes each foot dimension, such as FL holding the coordinate elements, $C_{FL,\ beginning}$ and $C_{FL,\ ending}$. This lets systems bridge the relationships between dimensions (see Figure 3), which can be simplified in the graphic diagram shown in Figure 4.

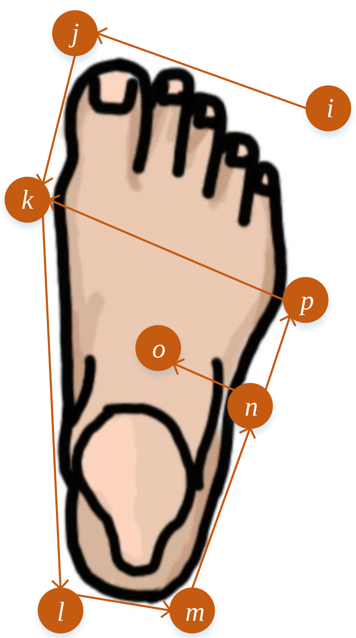

Figure 4. The graphic diagram of the foot-detection information stored in the G.

Figure 4 illustrates that each dimension is represented by two nodes (orange circles) and their edge (directed line), and that the node can play two roles, $\boldsymbol{C}_{i,\,beginning}$ and $\boldsymbol{C}_{i,\,ending}$, based on prior knowledge, as detailed in Equations (1) and (2). For instance, the element of $\boldsymbol{l}$ can be $\boldsymbol{k}_{BFL,\,ending}$ to connect $\boldsymbol{k}\rightarrow\boldsymbol{l}$, but it can be $\boldsymbol{m}_{HB,\,beginning}$ to connect $\boldsymbol{l}\rightarrow\boldsymbol{m}$. The graph-based algorithm helps systems flexibly detect the relationships, such as the indirect connection between $\boldsymbol{k}$ and $\boldsymbol{m}$ through the hidden node $\boldsymbol{l}$. The graph constitutes a powerful technology that lets systems be flexible in discovering missing information, using inference techniques to identify unknown relationships based on indirect connections.

In conclusion, graph $\boldsymbol{G}$ accumulates a semantic index based on nodes and their relationships and represents them in machine-readable formats, which are computable and ready to input into AR techniques. The following section will elaborate on how the $\boldsymbol{G}$ can produce meaningful information for visualizing feet in real-world applications.

4.3. Application Based on Feet Representation Using AR Techniques

This section aims to employ graph knowledge and represent it to general users. A LiDAR (a light detection and ranging sensor) is employed in our proposed application. It uses remote sensing with laser technologies to measure random objects quickly, which is suitable for real-time applications [27]. We employed the LiDAR sensor because it employs stable streaming to scan objects' surfaces and produce real-time laser signals to model foot shape references based on 3D objects [28]. The LiDAR has been built into Apple products, both on the iPhone and iPad, which are readily used by patients trying AR-based applications at home [29]. Our proposed application-based foot detection, using AR techniques, employed graph $\boldsymbol{G}$ from Section 4.2.

Algorithm 2 expresses how feet-detection systems extract information from graph $\boldsymbol{G}$, as shown in Figure 4. It computes the distance between V_1 and V_2 that model in 3D information (x, y, and z). The results from Algorithm 2 can be represented in AR applications, as shown in Figure 5.

Algorithm 2 Seven-foot Dimensions Representation

Inputs: foot graph′s graph, $\boldsymbol{G} = (\boldsymbol{V}, \boldsymbol{E})$

Outputs: a set of seven-foot dimensions, $\boldsymbol{D}$

1. **set** $\boldsymbol{D} = [\varnothing]$
2. **for each edge** $(\boldsymbol{V}_1, \boldsymbol{V}_2)$ **in** $\boldsymbol{G}$ **do**
3.   **set** $x_1, y_1, z_1 = \boldsymbol{V}_1$;
4.   **set** $x_2, y_2, z_2 = \boldsymbol{V}_2$;
5.   **set** $\|\boldsymbol{P}_i\| = 0$;
6. $\|\mathbf{P}_\mathrm{i}\| = \mathrm{sqrt}((\mathrm{x}_1 - \mathrm{x}_2)^2 + (\mathrm{y}_1 - \mathrm{y}_2)^2 + (\mathrm{z}_1 - \mathrm{z}_2)^2)$;
7.   add $\|\boldsymbol{P}_\mathrm{i}\|$ **to** $\boldsymbol{D}$;
8. **end for**
9. **return** $\boldsymbol{D}$;

Figure 5a shows how BFL dimension-based nodes are extracted from graph $\boldsymbol{G}$ and represented in the AR application. Figure 5b expresses the relationships between extracted nodes corresponding to our proposed seven-dimension models (see Section 4). Figure 5c illustrates that application-based feet detection using AR techniques helps non-expert users, such as diabetes patients, accurately measure their feet and visibly observe the real-time measurement results without requiring expert measurement devices.

The following section will prove that our proposed approach, based on seven-foot dimensions, can measure and simulate virtual shoe shapes and sizes that converge toward expert-based measurement.

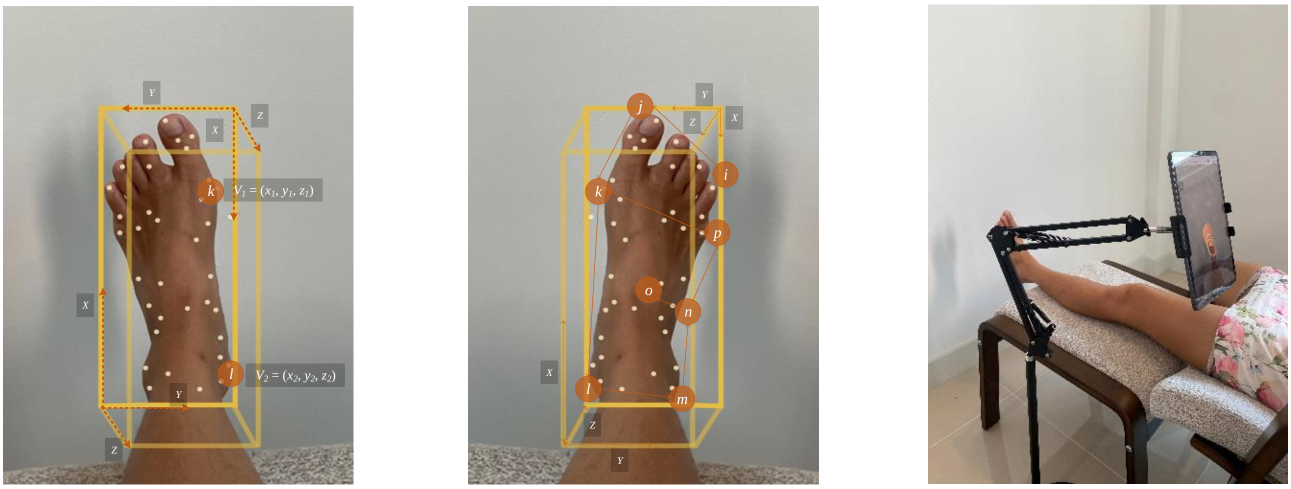

(**a**) (**b**) (**c**)

Figure 5. Example of a foot measurement based on AR technique. (**a**) BFL dimension-based node extraction; (**b**) Relation identification between dimension-based node; (**c**) The application-based feet detection using AR techniques.

5. Experimental Setup

In this section, we provide a detailed description of the experimental setup employed in our study. We evaluate the accuracy of the proposed foot detection system, present our experiments' results, and discuss their implications.

5.1. Experimental Objectives

Our research aims to evaluate the effectiveness of foot identification based on the seven-dimension model. This is because the accurate results of the system depend on how it identifies nodes and the relationships between them. Feet-measurement-based evaluations have three approaches: (1) the expert-based approach, (2) marker-based approach, and (3) sensor-based approach. The expert-based approach was considered because its results can be used as the gold standard to compare with our proposed approach and marker-based approach.

5.2. Data Set Description

The data were accumulated from field experiments between August 2022 and December 2022. Thirty volunteers (mean age $\pm$ SD: 26.80 $\pm$ 6.34 years) participated in the experiments and had no foot injuries or anomalies, including 13 females (mean age $\pm$ SD: 25.69 $\pm$ 6.52 years) and 17 males (mean age $\pm$ SD: 27.65 $\pm$ 6.26 years). Measuring foot shapes and sizes based on gender may be essential if basic foot template structures are employed. However, our proposed approach thoroughly extracts the key features, focusing on the seven-dimension model for general measurement without considering the physical effects based on gender difference.

The experiments followed the human research ethics authorized by the Office of the Human Research Ethics Committee of Walailak University (WU-EC-IN-1-003-65, approval date: 28 June 2022). The expert-based evaluation strictly followed the suggestions based on the proposed seven-dimension model. Each dimensional feature was measured two times to ensure the results were accurate. In this way, 1680 data points were employed to prove the effectiveness of foot identification.

5.3. Testing Metrics

The evaluation metrics for foot detection are precision, recall, and F-measure. They are the standard retrieval effectiveness metrics to measure how the proposed approach can recapture relevant dimensions against the expected results. Precision, recall, and F-measure are well-known evaluation metrics to measure the performance of automation systems for detection in clinical fields, as discussed by Dalianis, H. [30].

The expected results represent measurable outcomes from an expert-based approach; the accepted results from the proposed approach must converge to it, and the distance between them must be less than the gold standard (α). The α is set to 0.5 cm since the distance over it can be oversized or undersized and may cause subjects to be uncomfortable. The gold standard is employed by commercial sectors, as suggested by Adidas America, Inc. [31].

Precision represents the proportion of correctly detected dimensions against the total detected dimensions. The recall represents the proportion of correctly detected dimensions for all dimensions. F-measure is an overall accuracy that employs the harmonic mean of precision and recall. The measurements are defined as follows:

$$\text{precision} = \frac{\text{TP}}{\text{TP} + \text{FP}} \tag{3}$$

$$\text{recall} = \frac{\text{TP}}{\text{TP} + \text{FN}} \tag{4}$$

$$\text{f} - \text{measure} = \frac{2\times(\text{precision}\times\text{recall})}{\text{precision} + \text{recall}} \tag{5}$$

True positive (TP) is a correct outcome of the dimension that was evaluated (the distance $\leq \alpha$: suitable shape and size). False positive (FP) is an incorrect outcome of the dimension that was measured ($\alpha \leq$ the distance $\geq 2\alpha$: over or under shape and size). False negative (FN) is the expected outcome of the dimension that was not identified (the distance $\geq 3\alpha$: unknown shape and size).

5.4. Results and Discussions

The experiment considered the effectiveness of the proposed approach based on detection ability. It categorized the results into seven classes based on dimensions: FL, BFL, OBFL, FBD, FBH, HB, and IH. The marker-based approach and our proposed approach were judged regarding precision, recall, and F-measure. The effectiveness outcomes for seven-dimensions-based feet-detection approaches are shown in Table 2.

Table 2. The comparative effectiveness of seven-dimensions-based feet-detection approaches.

Approach	**Marker-Based Approach**			**Our Proposed Approach**		
Dimension	**Precision**	**Recall**	**F-Measure**	**Precision**	**Recall**	**F-Measure**
FL	0.46	0.65	0.54	0.37	0.77	0.50
BFL	0.46	0.87	0.60	0.63	1.00	0.78
OBFL	0.43	0.59	0.50	0.67	1.00	0.80
FBD	0.43	1.00	0.60	0.47	1.00	0.64
FBH	0.33	0.57	0.42	0.53	1.00	0.70
HB	0.63	1.00	0.78	0.63	1.00	0.78
IH	0.43	1.00	0.60	0.57	1.00	0.72
Average	**0.45**	**0.81**	**0.58**	**0.55**	**0.97**	**0.70**

According to Table 2, the marker-based approach produced a good average recall but poor average precision, which led to the average F-measure being unsatisfactory. Furthermore, its FBH and OBFL recalls are marginally unacceptable because it is good at detecting flat objects but less effective in detecting the depth of dimensions (varied over 2α and 3α), causing the results of FP and FN in the experiment. In contrast, the FBH F-measure is remarkably low, caused by poor precision and recall. FBH is a complex shape, and placing suitable markers is difficult. We may conclude that the marker-based approach is suitable for simple objects and not good enough for foot detection.

The average precision of our proposed approach is relatively low, because of high FP and since our algorithms detect dimensions based on the signals from LiDAR sensors. It holds a 1.00 cm resolution to determine complex objects, while our approach considers α as a 0.5 cm resolution. This causes some dimensions, such as FL and FBD, to be poor and suggestive. In contrast, the average recall of our proposed approach is outstanding, because our proposed approach is based on graph-based technologies with accurate signals from LiDAR sensors that could effectively address the FN in foot detection. This helps in achieving the acceptable average F-measure, and overall average precision and recall are thus higher than the marker-based approach. The summary of our findings based on the F-measure comparison is shown in Figure 6.

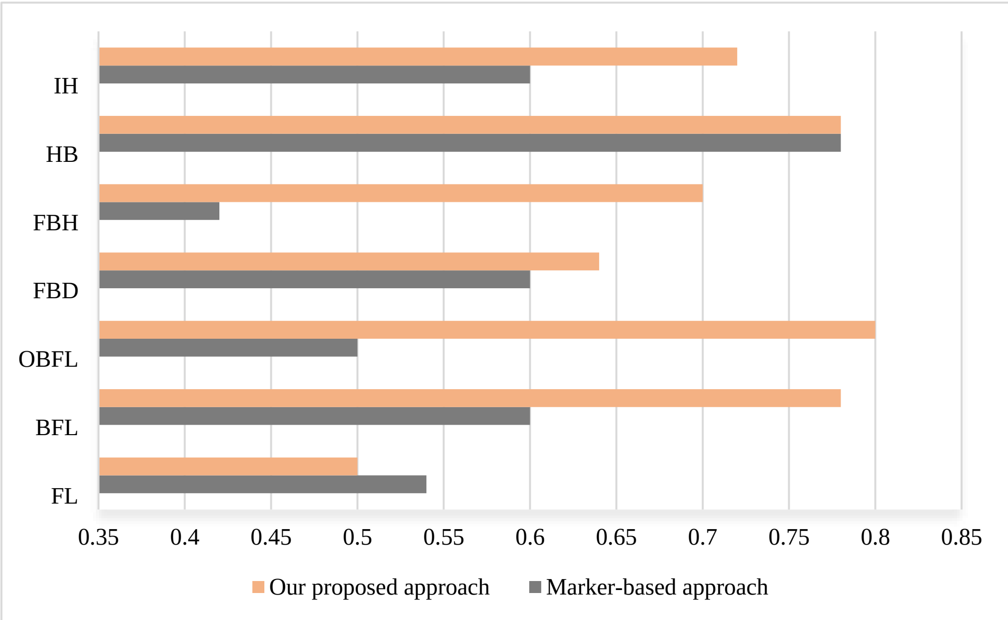

Figure 6. The F-measure comparison between the marker-based approach and our proposed approach.

Figure 6 illustrates the F-measure comparison using a histogram between the marker-based approach and our proposed approach; overall, our approach produces the highest values, such as OBFL, BFL, and FBH. We can interpret that our approach has great potential for helping the feet detection system accurately measure foot dimensions, converging to expert-like measurement. In other words, our proposed approach may help diabetes outpatients who need standardized and robust tools for foot measurement.

However, some dimensions, such as FL and FBD, still need to enhance their effectiveness, since their average precisions were lower than 70%. This challenge must be addressed using advanced algorithms, such as a deep learning approach to reduce FP problems, and using resampling techniques, such as those based on Markov chain Monte Carlo, to lower the number of FN with optimization algorithms.

6. Conclusions

This research has proposed designing and developing a foot-detection approach using the AR technique for virtual shoe try-on. The main contribution is the employment of the seven-foot dimensions model to measure foot shapes and sizes. The goal is to accurately detect the shapes and sizes in a real-time system. Our approach utilizes LiDAR, a real-time signal based on light detection and a ranging sensor, in order to identify foot shapes, sizes and surfaces, combined with our proposed graph-based representations of techniques, for the foot detection system.

Our approach was evaluated based on the effectiveness of foot dimension detection compared to the marker-based approach as the traditional technique. The results reveal that our approach yields a higher effectiveness than the traditional technique. Our proposed approach can accurately measure close to expert-like measurements and is suitable for susceptible patients sensitive to measuring foot shapes and sizes. This suggests it is the best-fit approach for real-time foot measurement applications, focusing on sensitive cases, that can be represented by a virtual try-on shoe system using the AR technique.

Our approach has recently been trained based on small samples in a particularly controlled environment, which can be interpreted as overfitting. In the future, we will organize in order to invite participants of a variety of ages, BMIs, medical histories, and sexes in order to discover how these impact foot measurement. Moreover, we may vary the experiment in different environments, such as in natural light during different periods and seasons, and apply noise techniques to help our approach become robust in unknown environments.

Author Contributions: Conceptualization, C.K.; methodology, C.K. and B.S.; software, C.K.; validation, C.K.; formal analysis, C.K.; investigation, C.K.; resources, C.K.; data curation, C.K. and B.S.; writing—original draft preparation, C.K.; writing—review and editing, B.S.; visualization, C.K.; supervision, P.B.; project administration, C.K.; funding acquisition, C.K. All authors have read and agreed to the published version of the manuscript.

Funding: This research was funded by the Research and Innovation Institute of Excellence, Walailak University (Grant No. WU64216).

Institutional Review Board Statement: The study was conducted in accordance with the Declaration of Helsinki, and approved by the Human Research Ethics Committee of Walailak University (protocol code WU-EC-IN-1-003-65, approval date: 28 June 2022).

Informed Consent Statement: Informed consent was obtained from all subjects involved in the study.

Data Availability Statement: None.

Conflicts of Interest: The authors declare no conflict of interest. The funder had no involvement in the research design, collection, analysis, writing, or interpretation.

References

1. Yang, P.; Shi, Y.; Li, S.; Tao, X.; Liu, Z.; Wang, X.; Wang, Z.L.; Chen, X. Monitoring the Degree of Comfort of Shoes In-Motion Using Triboelectric Pressure Sensors with an Ultrawide Detection Range. *ACS Nano* **2022**, *16*, 4654–4665. [CrossRef]
2. Yuan, M.; Li, X.; Xu, J.; Jia, C.; Li, X. 3D foot scanning using multiple {RealSense} cameras. *Multimed. Tools Appl.* **2020**, *80*, 22773–22793. [CrossRef]
3. Moore, Z.; Avsar, P.; Wilson, P.; Mairghani, M.; O'Connor, T.; Nugent, L.; Patton, D. Diabetic foot ulcers: Treatment overview and cost considerations. *J. Wound Care* **2021**, *30*, 786–791. [CrossRef]
4. Jurca, A.; Žabkar, J.; Džeroski, S. Analysis of 1.2 million foot scans from North America, Europe and Asia. *Sci. Rep.* **2019**, *9*, 19155. [CrossRef]
5. Shang, X.; Shen, Z.; Xiong, G.; Wang, F.-Y.; Liu, S.; Nyberg, T.R.; Wu, H.; Guo, C. Moving from mass customization to social manufacturing: A footwear industry case study. *Int. J. Comput. Integr. Manuf.* **2018**, *32*, 194–205. [CrossRef]
6. Maruyama, M.; Tabata, S.; Watanabe, Y.; Ishikawa, M. Multi-pattern Embedded Phase Shifting Using a High-Speed Projector for Fast and Accurate Dynamic 3D Measurement. In Proceedings of the 2018 IEEE Winter Conference on Applications of Computer Vision (WACV), Lake Tahoe, NV, USA, 12–15 March 2018.
7. Wu, G.; Li, D.; Hu, P.; Zhong, Y.; Pan, N. Automatic foot scanning and measurement based on multiple {RGB}-depth cameras. *Text. Res. J.* **2016**, *88*, 167–181. [CrossRef]
8. Banwell, H.A.; Paris, M.E.; Mackintosh, S.; Williams, C.M. Paediatric flexible flat foot: How are we measuring it and are we getting it right? A systematic review. *J. Foot Ankle Res.* **2018**, *11*, 21. [CrossRef]
9. Guo, K.; Xu, F.; Yu, T.; Liu, X.; Dai, Q.; Liu, Y. Real-time geometry, albedo and motion reconstruction using a single {RGBD} camera. *ACM Trans. Graph.* **2017**, *36*, 1. [CrossRef]
10. Paulo, M.M.; Rita, P.; Oliveira, T.; Moro, S. Understanding mobile augmented reality adoption in a consumer context. *J. Hosp. Tour. Technol.* **2018**, *9*, 142–157. [CrossRef]
11. Jiang, Q.; Sun, J.; Yang, C.; Gu, C. The Impact of Perceived Interactivity and Intrinsic Value on Users' Continuance Intention in Using Mobile Augmented Reality Virtual Shoe-Try-On Function. *Systems* **2021**, *10*, 3. [CrossRef]
12. Alkhamisi, A.O.; Monowar, M.M. Rise of Augmented Reality: Current and Future Application Areas. *Int. J. Internet Distrib. Syst.* **2013**, *01*, 25–34. [CrossRef]
13. Pachoulakis, I. Augmented Reality Platforms for Virtual Fitting Rooms. *Int. J. Multimed. Appl.* **2012**, *4*, 35–46. [CrossRef]

14. Saghazadeh, M.; Kitano, N.; Okura, T. Gender differences of foot characteristics in older Japanese adults using a 3D foot scanner. *J. Foot Ankle Res.* **2015**, *8*, 29. [CrossRef]
15. Alsheikh, S.; AlGhofili, H.; Alageel, R.; Ababtain, O.; Alarify, G.; Alwehaibi, N.; Altoijry, A. Diabetic Foot Care: A Screening on Primary Care Providers’ Attitude and Practice in Riyadh, Saudi Arabia. *Medicina* **2022**, *59*, 64. [CrossRef]
16. D'Angelo, G.; Della-Morte, D.; Pastore, D.; Donadel, G.; De Stefano, A.; Palmieri, F. Identifying patterns in multiple biomarkers to diagnose diabetic foot using an explainable genetic programming-based approach. *Future Gener. Comput. Syst.* **2023**, *140*, 138–150. [CrossRef]
17. Thotad, P.N.; Bharamagoudar, G.R.; Anami, B.S. Diabetic foot ulcer detection using deep learning approaches. *Sens. Int.* **2023**, *4*, 100210. [CrossRef]
18. Ahsan, M.; Naz, S.; Ahmad, R.; Ehsan, H.; Sikandar, A. A Deep Learning Approach for Diabetic Foot Ulcer Classification and Recognition. *Information* **2023**, *14*, 36. [CrossRef]
19. Mei, Z.; Ivanov, K.; Zhao, G.; Wu, Y.; Liu, M.; Wang, L. Foot type classification using sensor-enabled footwear and 1D-CNN. *Measurement* **2020**, *165*, 108184. [CrossRef]
20. Kini, K.R.; Madakyaru, M.; Harrou, F.; Sun, Y. Detecting pediatric foot deformities using plantar pressure measurements: A semi-supervised approach. *IEEE Des. Test* **2023**, 1-1. [CrossRef]
21. Chun, S.; Kong, S.; Mun, K.R.; Kim, J. A Foot-Arch Parameter Measurement System Using a RGB-D Camera. *Sensors* **2017**, *17*, 1796. [CrossRef]
22. Kim, J.H.; Kim, M.; Park, M.; Yoo, J. Immersive interactive technologies and virtual shopping experiences: Differences in consumer perceptions between augmented reality (AR) and virtual reality (VR). *Telemat. Inform.* **2023**, *77*, 101936. [CrossRef]
23. Serrano-Vergel, R.; Morillo, P.; Casas-Yrurzum, S.; Cruz-Neira, C. Exploring the Suitability of Using Virtual Reality and Augmented Reality for Anatomy Training. *IEEE Trans. Hum.-Mach. Syst.* **2023**, *53*, 378–389. [CrossRef]
24. Sip, P.; Kozłowska, M.; Czysz, D.; Daroszewski, P.; Lisiński, P. Perspectives of Motor Functional Upper Extremity Recovery with the Use of Immersive Virtual Reality in Stroke Patients. *Sensors* **2023**, *23*, 712. [CrossRef]
25. De Assis, G.A.; Brandão, A.F.; Correa, A.G.D.; Castellano, G. Characterization of Functional Connectivity in Chronic Stroke Subjects after Augmented Reality Training. *Virtual Worlds* **2023**, *2*, 1. [CrossRef]
26. Jeung, D.; Jung, K.; Lee, H.J.; Hong, J. Augmented reality-based surgical guidance for wrist arthroscopy with bone-shift compensation. *Comput. Methods Programs Biomed.* **2023**, *230*, 107323. [CrossRef]
27. Horváth, E.; Pozna, C.; Unger, M. Real-Time LIDAR-Based Urban Road and Sidewalk Detection for Autonomous Vehicles. *Sensors* **2021**, *22*, 194. [CrossRef]
28. Teppati Losè, L.; Spreafico, A.; Chiabrando, F.; Giulio Tonolo, F. Apple LiDAR Sensor for 3D Surveying: Tests and Results in the Cultural Heritage Domain. *Remote Sens.* **2022**, *14*, 4157. [CrossRef]
29. Luetzenburg, G.; Kroon, A.; Bjørk, A.A. Evaluation of the Apple iPhone 12 Pro LiDAR for an Application in Geosciences. *Sci. Rep.* **2021**, *11*, 22221. [CrossRef]
30. Dalianis, H. Evaluation Metrics and Evaluation. In *Clinical Text Mining*; Springer: Berlin, Germany, 2018; pp. 45–53. ISBN 9783319785035.
31. Adidas America, I. Men's and Women's Adidas Footwear Sizing. Available online: https://www.adidas.com/us/help/size_charts (accessed on 20 April 2023).